CHARACTERISTICS OF FLOW REVERSAL IN THE KINETIC REGIME

Yogi W. Budhi
Kelompok Keahlian Perancangan dan Pengembangan Proses,
Progam Studi Teknik Kimia, Fakultas Teknologi Industri, Institut Teknologi Bandung
Jl. Ganesha 10, Bandung 40132, Indonesia
E-mail : Y.Wibisono@che.itb.ac.id

Abstract

In principle, reactor perturbation by flow reversal can be used for manipulation of catalyst surface coverage if a dedicated and proper operation procedure can be developed. A mathematical model and analysis of reverse flow reactor behaviour for the ammonia oxidation over platinum have been performed. Series of reverse flow experiments were carried out on a laboratory reactor scale. The influence of flow reversals on the conversion and selectivity at various switching times was observed and evaluated. Other process variables such as gas residence time, reaction temperature, and oxygen concentration in the feed were points of interest. Assessment of reactor dynamics in the kinetic regimes can be achieved most expediently by implementing a comparable switching time and gas residence time. Model and experimental results indicate that regular reverse flow operation for manipulation of catalyst surface coverage always induces a decrease of conversion. It was also found that the selectivity due to flow reversal was rather insensitive to changes in the switching frequency.

Keywords : Ammonia oxidation, Kinetic regime, Reactor modeling, Residence time distribution, Reverse flow reactor operation, Transient operation

Abstrak

Pada dasarnya pertubasi reaktor oleh aliran balik dapat digunakan untuk mengatasi penutupan permukaan katalis manakala suatu suatu prosedur operasi yang spesifik dan sesuai bisa dibangun. Analisa dan model matematika kelakuan reaktor balik untuk oksidasi amoniak pada pelat platina telah dilakukan. Serangkaian percobaan aliran balik telah dilangsungkan dalam skala laboratorium. Pengaruh aliran balik terhadap konversi dan selektivitas pada berbagai jumlah putaran aliran telah diamati dan dievaluasi. Variabel proses lainnya, seperti waktu tinggal gas, temperature reaksi, dan konsentrasi oksigen pada umpan telah menjadi perhatian pada penelitian ini. Perkiraan dinamika reaktor dalam rejim kinetika umumnya dapat diperoleh melalui penelusuran implementasi jumlah putaran aliran dan waktu tinggal gas dengan perbandingan tertentu. Hasil percobaan dan pemodelan mengindikasikan bahwa operasi aliran balik reguler untuk memanipulasi penutupan permukaan katalis selalu mengakibatkan penurunan konversi. Selain itu, ditemukan juga bahwa selectivitas terhadap pembalikan aliran kurang sensitif terhadap perubahan pada frekuensi putaran aliran.

Keywords : Distribusi waktu tinggal, Operasi reaktor aliran balik, Operasi *transient*, Oksidasi amoniak, Pemodelan reaktor, Rejim kinetika

1. Introduction

Most chemical processes are usually designed to operate at a steady state condition. In practice, some process variables may vary with time, but the steady state design is based on the average values of these fluctuating quantities (Douglas and Rippin, 1966). Periodic reactor operation can in some cases produce more reaction products or a more valuable distribution of products than a steady state reactor (Silveston et al., 1995; Silveston, 1998). Moreover, transient methods have been suggested to study chemical kinetics experimentally (Bailey, 1973).

Among the various options for transient operation, the periodic mode offers the combined benefits of a permanent unsteady-state regime and a constant time-average regime. Periodically changing the flow direction through the reactor, better known as reverse flow operation (RFO), has not yet been widely applied for improvement of conversion or selectivity, but was shown beneficial for exothermic reactions from a viewpoint of energy saving (Boreskov et al., 1982; Boreskov and Matros, 1983; Matros and Bunimovich, 1996).

The use of the reverse flow principle as transient operation procedure for a catalytic reactor becomes interesting by the combination of dynamic properties at the microscale (catalyst) and at the macroscale (reactor). It may produce more favourable concentration and temperature profiles for the catalytic process (Ferreira et al, 1999).

Further developments of reverse flow operation yield novel concepts of reactor operation. Budhi et al. (2004) simulated the selective oxidation of ammonia in a reverse flow operation with temporarily lower feed concentration as a potential engineering manner for two reasons. First, the conversion decrease in regular reverse flow operation can be prevented. Second, the selectivity toward deep oxidation products can be significantly increased. However, this concept gives rise to a decrease of the production rate, which should be compensated by a larger reactor or parallel reactors.

Reverse flow operation with reactor side feeding is another way to avoid the conversion decrease in the regular reverse flow operation. This novel concept may also boost up the selectivity to deep oxidation products, while maintaining the production rate at a high level (Budhi et al., 2004b). A schematic illustration of a fixed bed reactor for reverse flow operation can be found elsewhere (Matros and Bunimovich, 1996; Budhi et al., 2004a).

In this contribution, possible operation procedures for an isothermal fixed bed reactor in reverse flow mode were experimentally studied in the kinetic regime with time periods to reverse the flow direction in the order of seconds. This is much less than the minutes to hours as used in the classical application of reverse flow operation for energy saving.

A first estimate of the switching time scale can be obtained from the ratio of the storage capacity of the catalyst and the feed flow rate of the reactant. It means that manipulation of the reactor selectivity requires considerably more frequent flow reversals in order to keep the catalyst surface in a dynamic state. If the reaction rate is fast compared to reversing the flow direction, then there is essentially a steady-state present for the reaction rate and corresponding catalyst surface coverages. If an antipode situation exists, then real unsteady-state behaviour holds for the system.

2. Fundamental

The catalytic fixed bed reactor was considered as a plug flow reactor and described with a heterogeneous model, distinguishing a gas phase and a catalyst phase. The source term includes the reaction rates on the basis of elementary reaction steps. The model complexity largely increases when the kinetics are involved on the level of elementary steps, which may induce highly non-linear behaviour. Flow reversal leads to transient behaviour, which means that the accumulation term should be incorporated in the continuity equations. The continuity equations for the gas phase and the solid phase used in this study were published before (Budhi et al., 2004a).

The current work uses the ammonia oxidation kinetics as developed by Rebrov et al. (2002) for Pt/Al_2O_3 catalyst, following work of Bradley et al. (1997), who observed that adsorbed oxygen, up to coverages of 0.35 mL, does not block the adsorption of ammonia. The experimentally obtained kinetic results were interpreted with a dual site mechanism. This means that nitrogen-containing species occupy one type of sites, so-called top sites, while non-nitrogen containing species occupy another type, known as hollow sites.

A new approach in developing the kinetic scheme states that adsorbed N itself can be considered in the hollow sites instead of top sites. According to experimental results on ammonia synthesis over Ru, adsorbed N residing in hollow sites was energetically favoured (Zhang et al., 2002). The elementary steps of the kinetic scheme and the reaction rate parameters were published before (Rebrov et al., 2002).

Steady state experiments were carried out with the set-up without any flow reversals to assess the reaction kinetics. Moreover, these data are

used as a basis to judge the potential of reverse flow operation procedures. Effects of reaction temperature, oxygen concentration, and gas residence time were observed during steady state experiments (Budhi, 2005). Steady state experiments were also performed in order to validate the kinetic model.

Some parameters of the kinetic model of Rebrov et al. (2002) were slightly adapted to provide accurate predictions for own experimental steady state data with respect to NH_3 and O_2 conversions, as well as the selectivities to N_2, NO, and N_2O. This is reasonable because the current catalyst, although Pt/Al_2O_3 as used by Rebrov et al. (2002), is not exactly the same. The platinum loading and the number of surface sites (obtained from CO chemisorption) were different. Moreover, the residence time of the gas in the reactors used was completely different as well. It is emphasized that the rate parameters of this study only show minor differences from the values reported by Rebrov et al (2002). Full data were reported (Budhi, 2005). In general the elementary step model seems adequate to describe the experimental data, meaning that it can be applied to describe reverse flow experiments.

3. Experimental set-up

The reverse flow reactor used in this work is a small-scale laboratory reactor. Transient data are obtained while alternating the flow direction. With the same set-up, steady state data were also obtained by operating the reactor in unidirectional flow.

The classical application of reverse flow, aiming at maximum energy saving, strives for a large temperature rise in the reactor. By consequence the reactor diameter should be relatively large as to avoid heat losses to the environment. In the application for selectivity manipulation as in the current work, the aspect of adiabatic operation seems less crucial, which would mean that a much smaller laboratory reactor could be applied. Focus was on the assessment of intrinsic kinetics and the subsequent study on how to apply those kinetics to see if RFO provides advantages. Therefore, it is not desired to disguise the kinetics by additional features like temperature and concentration gradients that might arise from mass or heat transfer limitation. Moreover, a plug flow pattern is desired as mixing causes a loss of kinetic influences. Pressure drop causes density and concentration changes, which again weaken the influence of kinetics. Various criteria from the literature such as pressure drop over the fixed bed reactor, plug flow requirement, axial and radial dispersions, and density variation were considered were considered in the fixed bed reactor design (Mears, 1971a; Froment and Bisschoff, 1990; Dautzenberg, 1994) in order to assess the kinetic regime. Although heat and mass transfer limitations are likely present in an industrial application, selectivity usually remains governed by kinetics.

A schematic view of the experimental set-up of reverse flow reactor is outlined in Figure 1 (Budhi, 2005). The set-up basically consists of a feed section, a reactor section, and an online gas analysis section. This set-up was designed with a fully automated control system. Labview software takes care of all data-acquisition and control actions. Since the set-up was computerized, opening and closing all solenoid valves at very short switching times, i.e. in the order of seconds, can be perfectly incorporated. Flow rates of the inlet gases were set with Brooks' mass flow controllers. A back-pressure controller was installed in order to perform the experiments at constant pressure, while for safety reasons, a pressure relief valve was present. Downstream the reactor just before the vent, a water condenser was installed to avoid condensation of the reaction product water in the vent system.

The feed section consists of six different gas lines, viz. NH_3, O_2, N_2, NO, N_2O, and He. Each line contains a pressure reducer, open/close valve, one-way valve, and a mass flow controller. Each gas can be supplied separately or in a mixture for calibration purposes. NH_3, O_2, and He mixtures are used as reactor feed during both steady state and reverse flow experiments. A static mixer (M-101, Figure 1) provides blending before entering the reactor.

The reactor section consists of preheaters (in-line resistance heating of each feed), a stainless steel fixed bed reactor, and a heated line behind the reactor. The preheaters are required to meet the desired inlet temperature; the heated outlet line is aimed to avoid water condensation. The reactor is contained in a fluidized sand bath to heat the reactor during the start-up and to maintain isothermal conditions during experiments.

The feed section ends up in two separate lines, one for each reactor inlet. The reactor ends can act as an inlet or an outlet, depending on the flow direction. The reactor is loaded with catalyst $Pt/-Al_2O_3$ retained by two sintered quartz plates. Sample chambers at both sides of the catalyst bed are connected via capillaries to the online mass spectrometer for real time analysis. A thermocouple tube allows monitoring the axial temperature profile along the catalyst bed. The total pressure in the reactor is kept constant at 1 bar and He is used as bulk gas.

The most crucial are the four-switching valves, which direct one feed to the reactor and stop the other feed. The valves are placed just behind the feed splitting point and in front of the feed gas preheater to avoid heat damage. The valves are alternately operated (two valves open, two valves closed) depending on the flow direction. For the reactor feed line where the valve is open, the feed gas passes a sort of checkvalve, consisting of a sapphire bead and spring release, just before it enters into the catalyst bed. A similar checkvalve is placed in the reactor outlet. To prevent gas outflow via the wrong outlet, a high pressure of helium is operated on that outlet to keep the sapphire bead in a close position. When the flow direction needs to change, the antipode situation holds.

The analysis section consists of an online mass spectrometer (VG Sensorlab 200D) both for steady state and transient measurements. The mass spectrometer measures NH_3 (m/e = 17), O_2 (m/e = 32), N_2 (m/e = 28), NO (m/e = 30), N_2O (m/e = 44), H_2O (m/e = 18), and He (m/e = 4) concentrations. Both the reactor inlet and outlet can be analyzed. Analysis of the gas is performed with a frequency of $120/n$ Hz, where n is the number of masses analyzed. Daily calibration of the mass spectrometer is required for obtaining quantitative data from the experiment. Detailed information about this mass spectrometer system has been reported before (Campman, 1996; Nievergeld, 1998; and Harmsen, 2001).

When reversing the flow direction of the feed, the sampling points to measure the product concentration need to switch. It is performed by using a 4-way sample valve, which allows the outlet gas sample to flow into the mass spectrometer, while the other one is flushed before being used for subsequent sampling. This valve works synchronously with the switching valves for reversing the flow direction. If desired, the sampling point can be fixed at one end of the reactor without switching the 4-way sample valve. In this condition, the mass spectrometer measures the inlet during one half-cycle and the outlet during the other half cycle. The PC-1 is used to monitor the online gas analysis and the PC-2 is used to operate and control the processes including all solenoid valves (Figure 1).

The experimental procedure for the selective oxidation of NH_3 can be described as follows, see Figure 1. Firstly, the water condenser (C-101) for cooling down the off-gas starts running. The reactor (R-101) is heated via the fluidized sand bath heater to the desired reaction temperature, while He (TP-07) flows through in one direction. Ammonia (TP-01) at certain concentration is introduced into the reactor when the reactor temperature has been reached, subsequently followed by O_2 (TP-06). The feed compositions can be set from the mass flow controllers (FIC-011 for NH_3, FIC-061 for O_2). Before entering the reactor, the feed gas mixture is blended in a static mixer (M-101). The preheaters (shown in traced line in front of the reactor) are installed near the reactor to gain the desired inlet temperature, which is approximately close to the reaction temperature.

The reaction products are continuously measured with the mass spectrometer. When the reactor attains steady state, which is indicated by the observed outlet concentrations, experiments under flow reversal can start. The flow direction is periodically reversed at every switching time, automatically induced by the computer (PC-2), using valves XV-103 and XV-102 for the inlets, XV-081 and XV-082 for the outlets. When the reactor stands by after completion of the daily experiments, a low He flow rate is maintained at a temperature of 373 K.

All experiments were carried out under conditions for intrinsic chemical kinetics when judged with well-known criteria as developed for steady state kinetic research (Mears, 1971a, 1971b; Rosendall and Finlayson, 1995). For the majority of data, the intrinsicity will not be affected by the applied transients (Hoebink et al., 1999), although this cannot be guaranteed shortly after switching the flow direction. Ammonia oxidation over alumina-supported platinum catalyst does not occur at temperatures below 473 K (Ostermaier et al., 1974, 1976). This is the reason to carry out the experiment in this study at distinct higher temperatures. The oxidation of ammonia in oxygen excess was studied in detail at temperatures below 653 K. In this case, it was reported by Sadykov et al. (2000) that there was no mass transfer limitation.

The catalyst 0.05% Pt on gamma alumina support as used in this work was provided by Unicore A.G. (Hanau). The catalyst particles were crushed and sieved to obtain a pellet size that minimizes theinfluence of intra particle diffusion. The catalyst was analyzed via CO chemisorption. Catalyst data, reactor specification, and typical operating conditions during the reverse flow experiments are shown in Table 1, unless otherwise indicated.

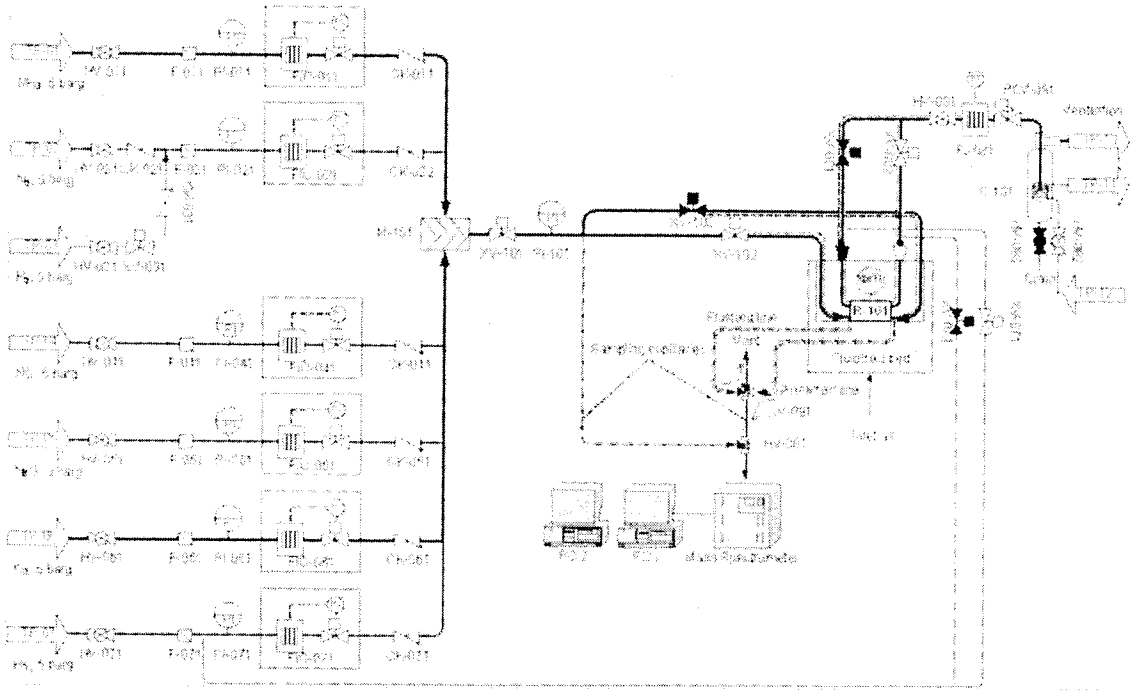

Gambar 4. Mekanisme Demixing Pembentukan Membran

Table 1. Catalyst, reactor properties, and operating conditions.

Total reactor length (m)	30×10^{-3}
Inner reactor diameter (m)	15×10^{-3}
Catalyst mass loaded (kg)	3.5×10^{-3}
Pt loading (%)	0.05
Capacity of catalyst (molsites kg^{-1}_{cat})	2.86×10^{-6}
Metal dispersion (%)	50
Metal surface area ($m^2\ kg^{-1}_{cat}$)	62
Catalyst pellet diameter (m)	$1.06\text{-}2.12 \times 10^{-4}$
Specific surface area ($m^2\ g^{-1}$)	93
Pore volume (BET, $cm^3\ g^{-1}$)	0.35
Catalyst pellet density ($kg\ m^{-3}$)	1230
Catalyst bulk density ($kg_{cat}\ m^{-3}_r$)	722
Bed porosity ($m^3_g\ m^{-3}_r$)	0.40
Switching time t_s (s)	2.5 – 30
Total pressure (bar)	1
Temperature (K)	523 – 673
Residence time τ (s)	0.3 – 0.9
NH_3 in feed (mol %)	1
O_2 / NH_3 ratio in feed	1 - 5

A fresh catalyst bed is heated under He flow by ramping the fluid bed temperature and the feed gas temperature at a rate of about 10 K per minute from room temperature to 773 K, which is 100 K higher than the maximum temperature planned for experiments. The catalyst is then gently oxidized by a stream containing 1 vol.% of O_2 in He, while the temperature during the catalyst pretreatment is maintained constant. The catalyst oxidation goes on for about 3 hours. Then the O_2 flow is stopped and the catalyst is kept under flowing He for about half an hour in order to purge reversibly adsorbed oxygen and other residual components. Finally, the catalyst is reduced with a 1 vol.% H_2 in He flow for 1 hour. The reactor is eventually allowed to cool down under He flow to the desired temperature of planned experiments by adjusting the feed gas temperature and the fluidized bed temperature.

It was found from introductory experiments that the catalyst exhibited a higher initial activity after daily start-up as compared to its activity after more than 3 hours time-on-stream. Significant deactivation during NH_3 oxidation over alumina-supported platinum catalyst was already reported in the literature (Ostermaier et al., 1974, 1976), and is due to catalyst saturation with reacting species. Therefore, a daily line-out procedure had to be carried out in order to minimize the influence of the reversible start-up effects on experimental results. Figure 2 shows the decay of the NH_3 conversion as function of time-on-stream after storage of the catalyst in a He stream. A profound decay takes place in about 3 hours, and afterwards the conversion remains fairly stable.

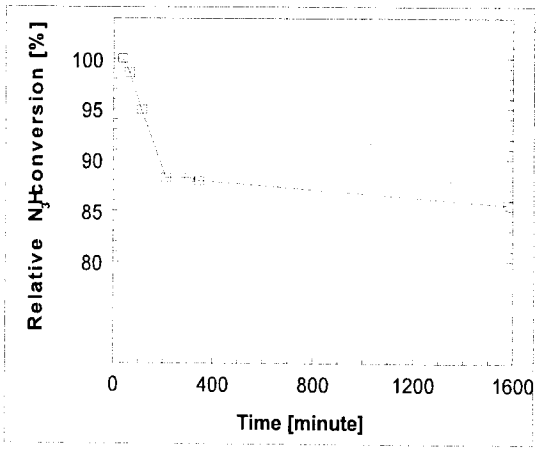

Figure 2. Relative ammonia conversion as a function of time-on-stream after catalyst storage in 5000 nml He/h at 373 K. Conditions: T = 573 K, feed NH_3 = 1 vol.%, O_2 = 5 vol.%, balance He. Total flow rate 10.000 nml/h, catalyst mass 3.5 g.

4. Results & Discussion

Figure 3 shows a typical transient profile of NH_3 as a function of time observed during regular RFO. During the periods of 0-15 s and 30-45 s, the profile of NH_3 corresponds with the inlet concentration, while during the period of 15-30 s, the outlet NH_3 concentration is monitored. The model can describe well the experimental result. Shortly after reversing the flow direction at 15 s, the concentration of NH_3 measured at the reactor outlet drops significantly and reaches the steady state level. The concentration of NH_3 increases again to the inlet level when the flow direction is reversed as can be seen at 30 s.

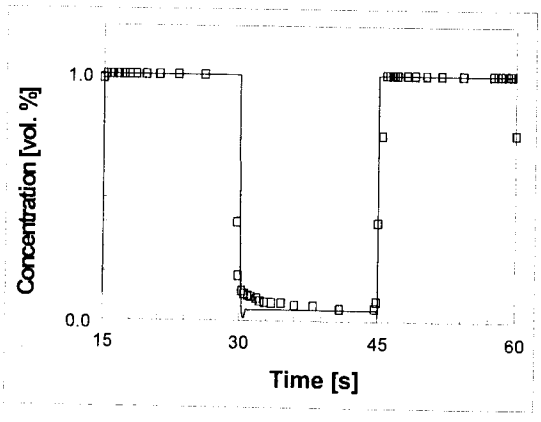

Figure 3. Concentration profile of NH_3 (markers) and model predictions (lines) as a function of time in regular RFO. Conditions: T = 673 K, t_s = 15 s, $_o$ = 0.6 s, FR = 1:1 in the feed, fixed sampling point.

As reported before (Budhi et al., 2004a), the ratio $t_s/_o$ determines whether RFO is in the quasi-steady state regime ($t_s/_o$ >> 1), in the dynamic regime ($t_s/_o$ 1), or in the sliding regime ($t_s/_o$ << 1). The dynamic regime seemed most promising for selectivity manipulation.

In the current series of experiments, the switching time was varied from 2.5 till 30 s, while the residence time was 0.6 s. It means that most experiments were done in the quasi-steady state regime, while the shorter switching times approach the dynamic regime. Switching times, shorter than 2 s, could not be applied due to limitations of the switching valves, mainly because of dead gas volumes in the lines. They would induce serious axial dispersion at the reactor inlet affecting the step-wise concentration changes. The high catalyst activity prevented to perform experiments at higher residence time.

Figure 4 shows model predictions and experimental results in terms of time-average conversion and selectivities versus switching time during regular reverse flow operation at 673 K and a 1:1 feed ratio (FR) of ammonia to oxygen. In order to allow a comparison of RFO and SSO, results are always expressed as differences between RFO and SSO data for conversion and selectivities. Similar results can also be seen in Figure 5, but for a temperature of 573 K and a feed ratio of ammonia to oxygen of 1:3.

The experimental data on the ammonia conversion and various selectivities demonstrate that the time-average values during RFO approach to the value in SSO if the switching time is very large. In regular RFO, the conversion of ammonia is always lower compared to the conversion in SSO. As should be expected, the decrease of ammonia conversion is more pronounced when the regime operation gradually shifts to the relaxed steady state (= shorter switching time) as also shown by the model predictions. At higher temperature (Figure 4) observed changes in conversion are larger than at lower temperature (Figure 5).

The decrease of the ammonia conversion during RFO is induced by different factors. First, the high concentration of ammonia near the reactor entrance is driven out when the flow direction is reversed. The low conversion of ammonia in that part obviously has a significant contribution to the time-average conversion of one complete cycle. The residence time of the gas that only reaches the beginning of the reactor is shorter than the residence time of the gas that penetrates further toward the reactor centre. Second, the amount of adsorbed oxygen on the catalyst surface has a distinct influence on the ammonia conversion

(Figure 6). Immediately after reversing the flow direction, the oxygen coverage suddenly occupies a high fraction of the surface. At $z = 1$, this fraction drops subsequently to a lower level before finally it reaches the steady state level. This profile behaviour shifts through the reactor in parallel with the flow direction as can be seen at $z = 0.5$ and $z = 0$. The decrease of the oxygen coverage at these positions is induced by the double trajectory of component oxygen when the flow direction is reversed. It means that the period of consuming adsorbed oxygen is longer. As a consequence, the conversion of NH_3 in RFO is lower than in SSO (Budhi et al., 2004a).

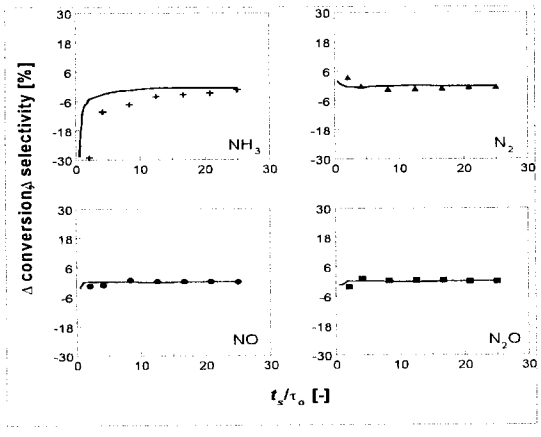

Figure 4. Experimental results (markers) and model predictions (lines) for NH_3 conversion and selectivities to N_2, NO, and N_2O as a function of switching time in regular RFO. Data are presented as difference between RFO and SSO. Conditions: $T = 673$ K, $_o = 0.6$ s, $FR = 1{:}1$.

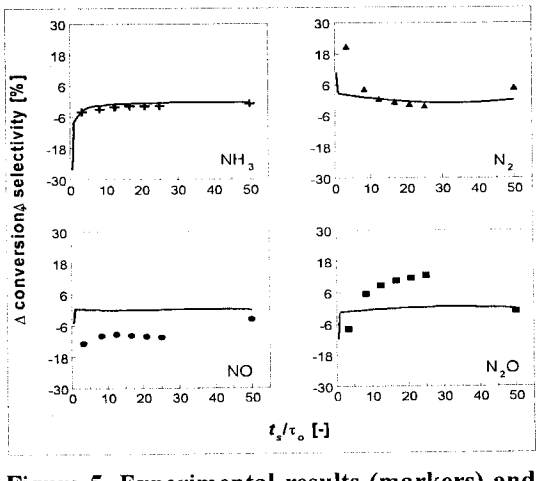

Figure 5. Experimental results (markers) and model predictions (lines) for NH_3 conversion and selectivities to N_2, NO, and N_2O as a function of switching time in regular RFO. Data are presented as difference between RFO and SSO. Conditions: $T = 573$ K, $_o = 0.6$ s, $FR = 1{:}3$.

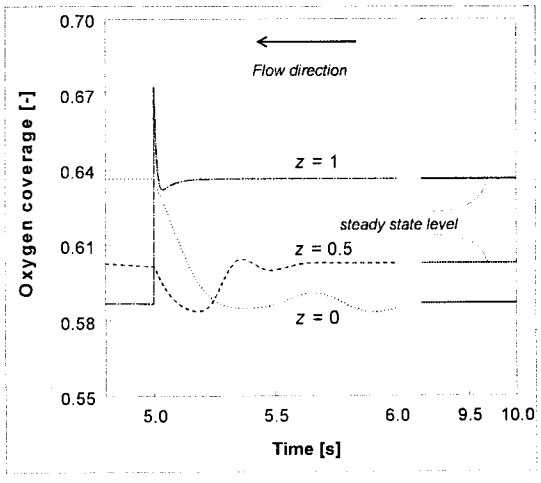

Figure 6. Model prediction of adsorbed oxygen coverage on the catalyst surface as a function of time in RFO. The horizontal levels show the SSO values. Conditions: $T = 573$ K, $_o = 0.6$ s, $FR = 1{:}1$, $t_s = 5$ s. The flow direction has changed at 5 s.

The observed selectivities at large switching times have similar values as observed during steady state operation, which should be expected. At short switching times the selectivity to N_2 exceeds the steady state levels, while the opposite holds for N_2O and NO (Figures 4 and 5). The effects are more pronounced in Figure 5, which concerns lower temperature and higher oxygen content of the feed. Here, at intermediate switching times, there is a distinct increase of the N_2O selectivity at the expense of the N_2 selectivity, while the NO selectivity remains at a clearly lower level in comparison to the steady state. Similar trends can be seen in Figure 4, but all effects are smaller.

Drawn curves in Figures 4 and 5 refer to model predictions. The NH_3 conversion changes, when comparing RFO and SSO, in Figure 4 are overestimated at low switching times. At lower temperature and higher oxygen content of the feed (Figure 5), model predictions and observation are in line. Selectivity predictions in Figure 4 are better than in Figure 5. In spite of the deviations in Figure 5, the model predicted trends follow the observations. With increasing switching time, the N_2 selectivity decreases down to a minimum value, and then slightly increases to the quasi-steady state value. Similarly the N_2O selectivity increases up to a maximum before reaching the steady state level, as is in line with the trend of the data. In Figure 4 model predictions follow the trend of the data as well. Here, it seems that quasi-steady state values of the selectivity changes are reached at shorter switching time than occurs in Figure 5.

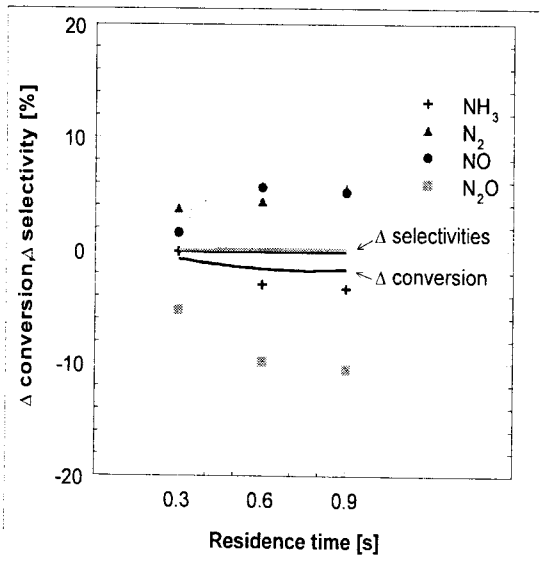

Figure 7. Experimental results (markers) and model predictions (lines) for NH_3 conversion and selectivities to N_2, NO, and N_2O as a function of residence time in regular RFO. Data are presented as difference between RFO and SSO. Conditions: T=573 K, FR=1:3, t_s=5 s.

Figure 7 presents experimental results for NH_3 conversion and selectivities to N_2, NO, and N_2O as a function of the residence time in regular RFO. An increase of the residence time at constant switching time induces a larger decrease of the ammonia conversion difference between RFO and SSO, which trend is confirmed by the model prediction. Increasing the residence time at constant switching time relatively shifts the operation more towards the sliding regime. Even if the operation regime might be still in the quasi-steady state, such movement will contribute to the decrease of conversion, which is more pronounced when switching time over residence time is smaller. It was previously mentioned that the conversion of ammonia in the sliding regime in regular RFO is always lower than in SSO.

The selectivity to N_2O decreases if the residence time increases, while the selectivities to N_2 and NO increase. The model predicts that the product distribution would not change because the operation regime is still in the quasi-steady state. Besides the switching time, the temperature has a significant influence. Figure 8 depicts the effect of temperature on the conversion and selectivity differences when reverse flow operation and steady state operation are compared. At 673 K, the change of the ammonia conversion is more pronounced than at 573 K. In contrary, the product distribution differences between reverse flow and steady state operations are rather minor at 673 K. Increasing the temperature obviously causes the reaction rates to increase, while the dynamic influence due to flow reversal becomes less, which might lead to a stronger influence on the conversion of unconverted reactants after a flow reversal. A similar behaviors is also seen when comparing Figures 4 and 5, albeit that there exists a difference in the NH_3/O_2 ratio as well between these figures. But the higher temperature of Figure 4 suggests to induce that the quasi-steady state regime is already observed at smaller ratios of the switching time over residence time. Ideally, to reduce the decrease of ammonia conversion due to the faster reaction rate at higher temperature, the switching time should be set at reasonably larger time periods.

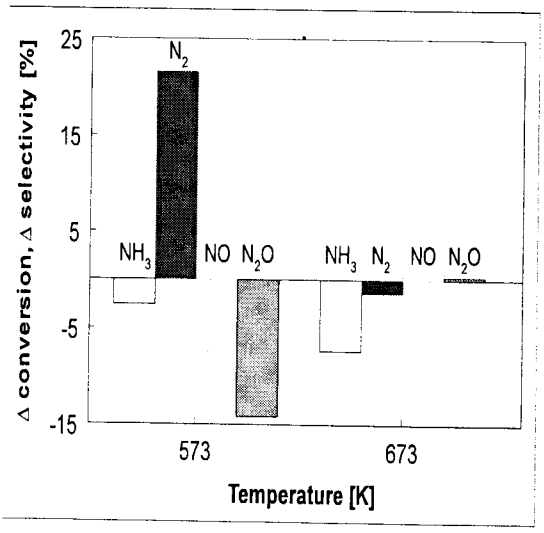

Figure 8. Experimental results for NH_3 conversion and selectivities to N_2, NO, and N_2O as a function of temperature in regular RFO. Data are presented as difference between RFO and SSO. Conditions: $_a$=0.6 s, FR=1:1, t_s=5 s.

The selectivity differences between reverse flow operation and steady state operation become less at 673 K compared to 573 K. This is in line with simulations showing that at even higher temperature the product distribution changes due to flow reversal are minor. The results of Figures 4 and 5 confirm this point as well. As the reactions proceed at larger rate, the dynamics of the reactor relatively tend to decrease as effectuated by smaller deviations from the steady state conditions. Effects of temperature on the product distribution as expected during steady state operation are still present in this case, where the selectivity to N_2 decreases and selectivities towards NO and N_2O go up at higher temperature.

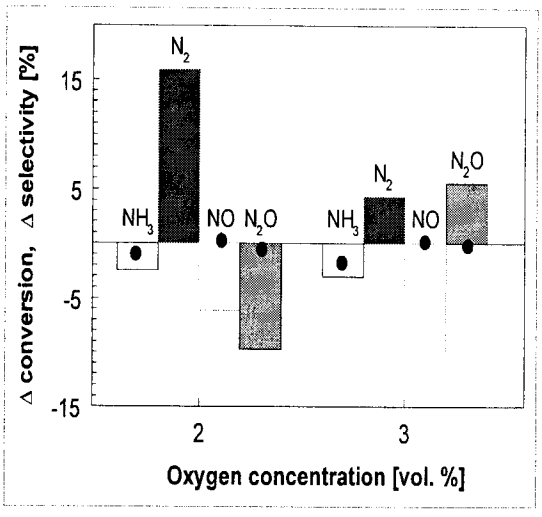

Figure 9. Experimental results for NH_3 conversion and selectivities to N_2, NO, and N_2O as a function of oxygen concentration in regular RFO. Conditions: T = 573 K, $_{o}$ = 0.6 s, FR = 1:2 and 1:3, t_s = 5 s. The dots show the model prediction.

Figure 9 illustrates the effect of the oxygen feed concentration on the NH_3 conversion and selectivities to N_2, NO, and N_2O. The conversion of ammonia is hardly changed by increasing the oxygen concentration from 2 vol.% to 3 vol.% because it has already reached a high level during the steady state operation. With increasing oxygen concentration, the difference in conversion between RFO and SSO is slightly larger because the conversion increase in SSO is higher than in RFO. The model prediction of difference of the NH_3 conversion also decreases when the oxygen concentration is higher. However, the model prediction slightly overestimates the experimental result. The changes of the selectivity (RFO-SSO) towards N_2 decrease when increasing the oxygen feed concentration. At higher oxygen concentration, a higher oxygen surface coverage would stimulate the production of oxygen containing products as to be expected in SSO. This trend is confirmed by the selectivity changes with respect to N_2O, which turn from negative to positive when the oxygen feed content increases. For NO the selectivity changes become more negative. The product distribution for steady state operation favours N_2 and N_2O at 573 K. The model predictions, as indicated by the dots in Figure 9, show smaller effects than observed experimentally, but the trend of the predictions follows the data.

An asymmetric switching time is another option when exploring the behaviour of reverse flow operation from a viewpoint of selectivity manipulation. It can be performed by applying a different time period between forward and backward flows ($t_{s,}$ $t_{s,}$, but $t_{s,} + t_{s,} = t_c$). In principle, such kind of operation procedure may create other unique coverages of the active sites because the profile development of the adsorbed species along the reactor is different for the two flow directions. The real phenomena that occur during the operation are more complicated due to the fact that a lot of process variables are involved. In this study, observation was focused on two different switching times, i.e. at t_s = 2.5 s and t_s = 5 s. The comparison between symmetric and asymmetric RFO is given in Table 2.

As can be seen, the conversions of NH_3 indicate a lower value during asymmetric RFO than during symmetric RFO for both cases. It means that the shorter time period, i.e. 25% of cycle time, in asymmetric RFO might contribute more significantly to the decrease of the NH_3 conversion, which results in a lower overall conversion. In both cases, the selectivity changes towards each component are slightly less for asymmetric RFO than for the symmetric RFO case.

Table 2. Experimental results of NH_3 conversion and selectivities to N_2, NO, and N_2O for symmetric and asymmetric regular RFO. The switching time during symmetric RFO is the same, 50% of cycle time for each flow direction, while during asymmetric RFO it is 25% and 75% of cycle time for left to right and for right to left, respectively. Conditions: T = 673 K, $_{o}$ = 0.6 s, FR = 1:5.

	t_s = 2.5 s			t_s = 5 s	
	Symmetric	Asymmetric		Symmetric	Asymmetric
Δ conversion of NH_3, %	-15.0	-28.4		-8.5	-22.7
Δ selectivity to N_2, %	+11.6	+10.7		+9.3	+9.2
Δ selectivity to NO, %	-12.9	-10.8		-11.0	-9.4
Δ selectivity to N_2O, %	+1.3	+0.01		+1.7	+0.2

5. Conclusion

A study was made about reverse flow operation at switching times in the order of seconds, which are required for selectivity manipulation via reverse flow operation. A switching time close to the gas residence time is typically required. Regular reverse flow operation always invokes a conversion decrease as observed from experiments and model predictions. This major drawback of regular RFO is most pronounced at shorter switching time. It was also found that the selectivity was rather insensitive to changes in the switching frequency at high temperature, but distinctly different selectivities were observed at lower temperature. An increase of the gas flow rate at constant switching time basically shifts the operation regime towards the relaxed steady state. The reaction temperature and the oxygen concentration may affect the conversion and selectivity in RFO, which effect might be positive or negative, depending on their relative influence. Asymmetric RFO induces an even larger conversion decrease, while it may influence the product distributions.

In order to prevent the conversion decrease in regular RFO, a novel concept of reverse flow operation is indispensable. This topic will be presented in Part 2 (Budhi et al., upcoming paper), so called reverse flow operation with temporarily lower feed concentration.

Notation

$E(t)$ = residence time distribution function (s^{-1})
F = volumetric flowrate ($m^3_{gas}\,s^{-1}$)
FR = concentration feed ratio of NH_3 to O_2 (-)
T = temperature (K)
t = time (s)
t_c = cycle time (s)
t_s = switching time (s)
V_r = reactor volume ($m^3_{reactor}$)
z = dimensionless axial position (-)

Greek letters

ε_b = bed porosity ($m^3_{gas}\,m^{-3}_{reactor}$)
Δ = conversion or selectivity difference between RFO and SSO
τ_0 = gas residence time in once-through operation (s)

Subscripts

H = time period at high concentration
L = time period at low concentration
$\rightarrow$ = flow direction to right
$\leftarrow$ = flow direction to left

Acknowledgement

The financial support, provided by Novem (the Netherlands Agency for Energy and Environment), STW (Dutch Technology Foundation), and Quality for Undergraduate Education Project, Chemical Engineering Department, Institute of Technology Bandung, Indonesia, was gratefully acknowledged during this PhD research at Technische Universiteit Eindhoven, the Netherlands under supervisors Prof.dr.ir. J.C. Schouten and dr.ir. J.H.B.J. Hoebink (r.i.p.).

Daftar Pustaka

[1.] Bailey, J.E., 1973. Periodic operation of chemical reactors: a review. Chemical Engineering Communication 1, 111-124.

[2.] Boreskov, G.K., Bunimovich, G.A., Matros, Yu.Sh., Ivanov, A.A., 1982. Catalytic processes under non-steady state conditions. II. Switching the direction for the feed of the reaction mixture to the catalyst bed. Experimental results. Kinetic and Catalysis 23 (2), 402-406.

[3.] Boreskov, G.K., Matros, Yu.Sh., 1983. Unsteady-state performance of heterogeneous catalytic reactions. Catalysis Review Science and Engineering 25, 551-590.

[4.] Bradley, J.M., Hopkinson, A., King, D.A., 1997. A molecular beam study of ammonia adsorption on Pt{100}. Surface Science 371, 255-263.

[5.] Budhi, Y.W., 2005. Reverse Flow Reactor Operation for Control of Catalyst Surface Coverage. Ph.D. Dissertation, Technische Universiteit Eindhoven, the Netherlands.

[6.] Budhi, Y.W., Hoebink, J.H.B.J., Schouten, J.C., 2004b. Reverse flow operation with reactor side feeding: Analysis, modeling, and simulation. Industrial and Engineering Chemistry Research 43, 6955-6963.

[7.] Budhi, Y.W., Jaree, A., Hoebink, J.H.B.J., Schouten, J.C., 2004a. Simulation of reverse flow operation for manipulation of catalyst surface coverage in the selective oxidation of ammonia. Chemical Engineering Science 59, 4125-4135.

[8.] Campman, M., 1996. Kinetics of Carbon Monoxide Oxidation over Supported Platinum Catalytsts. The Role of Steam in the Presence of Ceria. Ph.D. Dissertation, Technische Universiteit Eindhoven, the Netherlands.

[9.] Dautzenberg, F.M., 1994. Selected Topics from Applied Industrial Catalysis. Ph.D. Dissertation, Technische Universiteit

Eindhoven, the Netherlands.

[10.] Douglas, J.M., Rippin, D.W.T., 1966. Unsteady state process operation. Chemical Engineering Science 21, 305-315.

[11.] Ferreira, R.Q., Costa, C.A., Masetti, S., 1999. Reverse-flow reactor for a selective oxidation process. Chemical Engineering Science 54, 4615-4627.

[12.] Froment, G.F., Bischoff, K.B., 1990. Chemical Reactor Analysis and Design, 2nd ed., Wiley.

[13.] Harmsen, J.M.A., 2001. Kinetic Modelling of the Dynamic Behaviour of an Automotive Three-Way Catalyst under Cold-Start Conditions. Ph.D. Dissertation, Technische Universiteit Eindhoven, the Netherlands.

[14.] Hoebink, J.H.B.J., Nievergeld, A.J.L., Marin, G.B., 1999. CO oxidation in a fixed bed reactor with high frequency cycling of the feed. Chemical Engineering Science 54, 4459-4468.

[15.] Matros, Yu. Sh., Bunimovich, G. A., 1996. Reverse-flow operation in fixed bed catalytic reactors. Catalysis Review Science and Engineering 38, 1-68.

[16.] Mears, D.E., 1971a. Diagnostic criteria for heat transport limitations in fixed bed reactors. Journal of Catalysis 20, 127-131.

[17.] Mears, D.E., 1971b. The role of axial dispersion in trickle-flow laboratory reactors. Chemical Engineering Science 26, 1361-1366.

[18.] Nievergeld, A.J.L., 1998. Automotive Exhaust Gas Conversion: Reaction Kinetics, Reactor Modelling and Control. Ph.D. Dissertation, Technische Universiteit Eindhoven, the Netherlands.

[19.] Ostermaier, J.J., Katzer, J.R., Manogue, W.H., 1974. Crystallite size effects in the low-temperature oxidation of ammonia over supported platinum. Journal of Catalysis 33, 457-473.

[20.] Ostermaier, J.J., Katzer, J.R., Manogue, W.H., 1976. Platinum catalyst deactivation in low-temperature ammonia oxidation reactions: I. Oxidation of ammonia by molecular oxygen. Journal of Catalysis 41, 277-292.

[21.] Rebrov, E.V., de Croon, M.H.J.M., Schouten, J.C., 2002. Development of the kinetic model of platinum catalyzed ammonia oxidation in a microreactor. Chemical Engineering Journal 90, 61-76.

[22.] Rosendall, B., Finlayson, B.A., 1995. Transport effects in packed-bed oxidation reactors. Computer and Chemical Engineering 19, 1207-1218.

[23.] Sadykov, V.A., Isupova, L.A., Zolotarskii, Bobrova, L.N., Noskov, A.S., Parmon, V.N., Brushtein, E.A., Telyatnikova, T.V., Chernyshev, V.I., Lunin, V.V., 2000. Oxide catalyst for ammonia oxidation in nitric acid production: properties and perspective. Applied Catalysis A 204, 59-87.

[24.] Silveston, P.L., 1998. Composition Modulation of Catalytic Reactors, Ontario, Canada: Gordon and Breach.

[25.] Silveston, P.L., Hudgins, R.R., Renken, A., 1995. Periodic operation of catalytic reactors - introduction and overview. Catalysis Today 25, 91-112.

[26.] Zhang, C.J., Lynch, M., Hu, P., 2002. A density functional theory study of stepwise addition reactions in ammonia synthesis on Ru(0 0 0 1). Surface Science 496, 221-230.